Microfluidics and Nanofluidics (2019) 23:127
https://doi.org/10.1007/s10404-019-2294-y

REVIEW

Beyond high voltage in the digital microfluidic devices for an integrated portable sensing system

Xin Min[1] · Woo Soo Kim[1]

Received: 23 June 2019 / Accepted: 17 October 2019 / Published online: 29 October 2019

Abstract
Digital microfluidics (DMFs) show great potential in the fields of lab-on-a-chip applications for electro-chemical as well as biochemical sensing for decades. Various types of DMF devices have been demonstrated to improve their capabilities such as smaller device size for portability, higher reliability, and multi-purpose applications, etc. Among them, the electrowetting on dielectric (EWOD) is one of the most widely used mechanisms to manipulate droplets due to its good flexibility. On the other hand, the high-voltage application that required for EWOD-type DMF also limits the portability and dimension of the whole system. In this review, we discuss the DMFs which are powered by alternative sources other than electrical sources and evaluate their potential for future portable biochemical assays. Then, the demonstrations reported with the possibility beyond high voltage are discussed starting from lowering voltage requirement for EWODs to the unique methods using mechanical, optical, and energy harvesting to power DMF devices. Finally, the practical applications and prospective on the integrated multi-functional lab-on-a-chip applications are tackled.

Keywords Digital microfluidics · Portable platforms · Sensing system · Energy efficient

1 Introduction

Recently, advanced microfluidic devices have attracted significant attention for their applications which minimize conventional progressive laboratory activities to a chip-level system (Mijatovic et al. 2005; Whitesides 2006). The application of microfluidic devices not only largely shrink the sample size that required for chemical and biological reactions, but also enable remote test without giant laboratory equipment (Wainright et al. 2003; Dittrich and Manz 2005). The most commonly used microsystem relies on continuous microflows passing through channels to carry and transport a single droplet (Mcdonald et al. 2000). The reduction of sample and reagent size also brings the benefit of lower cost and control of hazardous materials (Ng et al. 2002). To be used as a point-of-care biochemical system, this platform usually requires another immiscible liquid to carry the droplets, which brings many external modules and complicated fabrication process (Beebe et al. 2002). In addition, the function of most of the platforms is confined to a certain type, which cannot be used for multi-function usage. Comparing to this continuous fluid-based microfluidic channel, digital microfluidics (DMFs) emerged as a novel tool to manipulate droplets in a discrete, precise, and single-phase way (Gong and Kim 2008; Fan et al. 2009; Park et al. 2010a). The configuration of DMFs enables concise integration of the whole system without tedious pumps and valves which are usually required for traditional microfluidic devices (Wang and Jones 2015). Also, the DMF system enables droplets automation control for multiple steps assays (Hadwen et al. 2012).

Different DMF actuation mechanisms have been reported such as electrowetting on dielectric (EWOD) (Tan et al. 2012), mechanical motion (Darhuber et al. 2003), surface acoustic wave (SAW) (Beyssen et al. 2006), and optical (Chiou et al. 2003) methods. Among them, the EWOD-type device is the most widely used due to its high flexibility and easy fabrication process (Yafia et al. 2015b), which can be integrated with multiple functions. Figure 1a shows the general open configuration of EWOD before and after the change of contact angle (Jain et al.

✉ Woo Soo Kim
woosook@sfu.ca

[1] Additive Manufacturing Laboratory, School of Mechatronic Systems Engineering, Simon Fraser University, Surrey, BC V3T 0A3, Canada

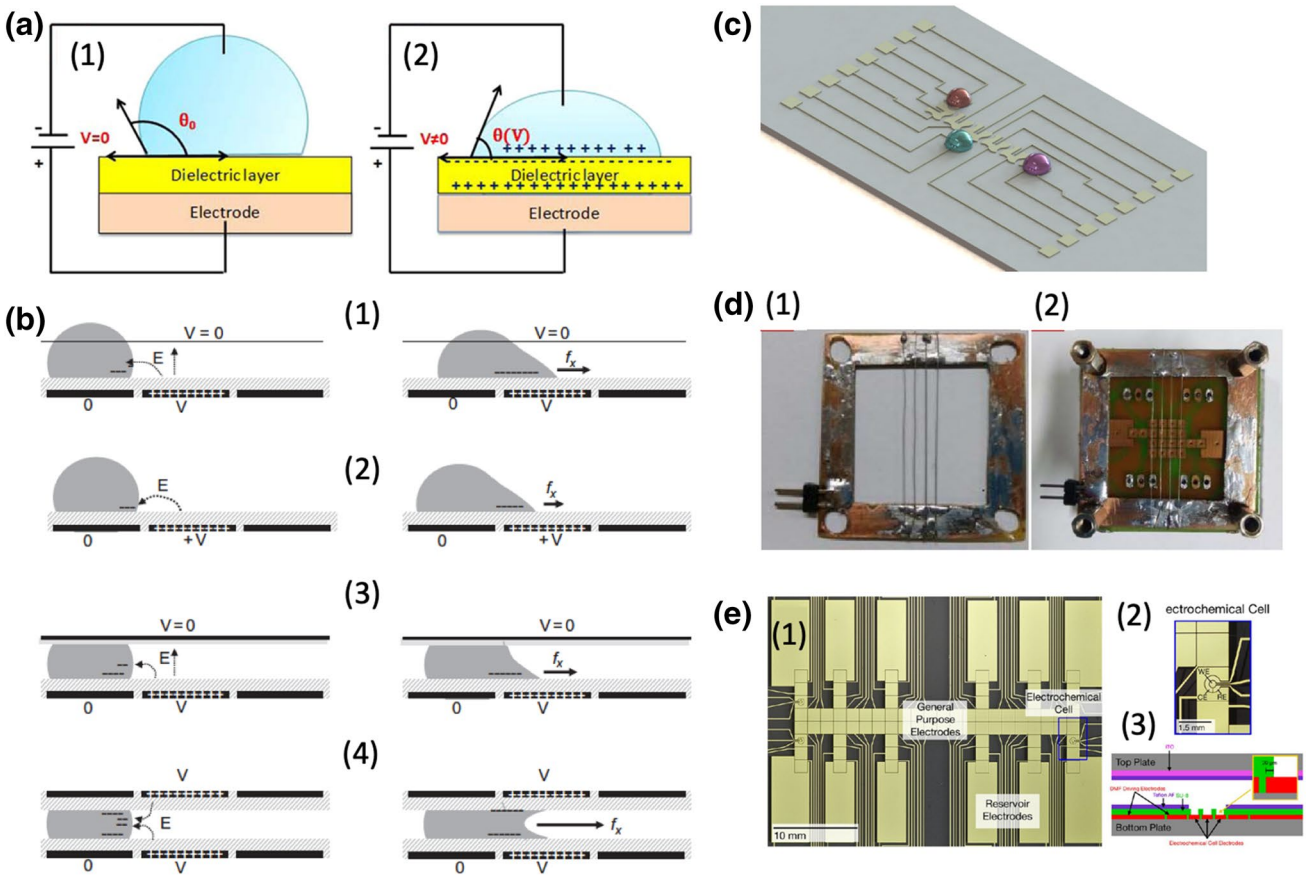

Fig. 1 **a** Mechanism of electrowetting on dielectric (EWOD). (1) The droplet exhibits a large contact angle when there is no voltage applied. (2) The contact angle decreased after the voltage is applied and the droplet looks like "wetted" on the dielectric surface (Jain et al. 2017c). **b** Different configurations of digital microfluidics (DMFs). (1) open DMF with catena. (2) Open type DMF. (3) Close DMF with the uniformed ground top plate. (4) Close type DMF with double electrodes (Berthier 2013). **c** An open type DMF whose electrodes are fabricated on glass slides via the additive manufacturing process (Min et al. 2019). **d** A 2D-arranged open type DMF with catena (Jain et al. 2017b). **e** Close type DMF with reservoirs and sensing areas integrated on the platform (Dixon et al. 2016)

2017c). Briefly, the wetting behavior of the droplet obeys Lipmann–Young's equation:

$$\cos\theta(V) = \cos\theta_0 + \frac{\varepsilon_r \varepsilon_0}{2d\gamma} V^2, \tag{1}$$

where V is the voltage applied, ε_r and ε_0 are the relative dielectric constant and permittivity of free space, d is the dielectric thickness, γ is the surface tension between solid and liquid, θ_0 and θ are the contact angle before and after voltage applied. Figure 1b demonstrates four different common designs of EWOD devices which can be categorized into open and closed configurations (Berthier 2013). Each of these different types has its own advantages and disadvantages. Comparing to open type, the configuration of close type devices is more complicated and own high viscous resistance, but it can decrease the evaporation rate of tiny droplets and control the droplet size more precisely through on-chip reservoirs (Islam and Tong 2017). Electrodes are usually fabricated on a substrate through the photolithography method, following the process of dielectric and hydrophobic layer coating, where spin-coating is commonly used (Wang et al. 2016). Some of the studies also exhibit the potential of other fabrication methods including additive manufacturing (Min et al. 2019), screen printing (Monkkonen et al. 2016), and inkjet printing (Dixon et al. 2016) for future low-cost and mass production purpose. Several types of DMF devices fabricated through different methods have been shown in Fig. 1c–e. A generally designed 2D array of electrodes enables this platform to perform complicated parallel operations and to be integrated with different functions (Grissom et al. 2015; Yu et al. 2017).

Despite the success achieved by EWOD-type DMFs, these devices also suffered from some certain drawbacks including a large voltage control unit required to manipulate the droplet, and a limited number of electrodes and wire connections (Wang et al. 2017a). The high voltage, which is usually hundreds of volts, required to drive droplets also

brings potential safety issues and confines the application of this platform. Efforts have been devoted to lowering the electrowetting voltage to several volts level. To obtain better actuation functionality, high dielectric constant materials have been used to decrease the voltage requirement for the same contact angle change (Moon et al. 2002). Also, the theory of electrode geometry design has been developed to eliminate failure movement and further lower the driving voltage (Datta et al. 2016; Pooyan and Passandideh-Fard 2018). On the other hand, a lot of studies explore the possibility of alternative powering sources other than applying voltage to drive the droplets (Park et al. 2010b; Zhang et al. 2011; Chiou et al. 2013). Although these types of DMF devices are less popular than EWOD, their uniqueness still needs to be emphasized. This review first focuses on the progress that has been reported to lower the voltage requirement for EWOD, which contains opportunities of using new materials during the fabrication process and explores better design of electrode geometry. Then, DMF devices based on four different droplet driving mechanisms have been introduced and compared with conventional EWOD. It is worth to mention that all these different types of devices not only have their own unique advantages and applications, but also suffer from certain drawbacks. The goal of this review was to evaluate the potential of different types of DMF platforms other than EWOD for reliable and energy-efficient lab-on-a-chips. Then, we summarize the unique applications of these DMFs and their perspectives as integrated point-of-care devices.

2 Toward lowering the power for EWOD

2.1 Using high dielectric constant materials

As shown in Eq. (1), the contact angle change in EWOD is governed by (1) the dielectric constant, (2) thickness of the dielectric layer, (3) surface tension between different phases, and (4) the voltage applied on the electrodes. Under the same ambient environment, to achieve the same contact angle change with lower voltage, we can either increase dielectric constant or decrease the thickness. However, the thickness of the dielectric layer cannot be too thin because of the breakdown effect when applying high voltage (Chang et al. 2010; Rudan 2015; Mibus et al. 2016). Hence, using high dielectric constant materials becomes a better and reliable choice.

Barium strontium titanate (BST) became a good candidate as dielectric layer material in the EWOD application as early as 2002 (Moon et al. 2002). The extremely large dielectric constant (~ 180) enables BST to be fabricated into a very thin layer without damage after applying high voltage (Wang et al. 2017b), which further enhances the contact angle change of the droplet. A contact angle change of 40° only with 15 V has been demonstrated

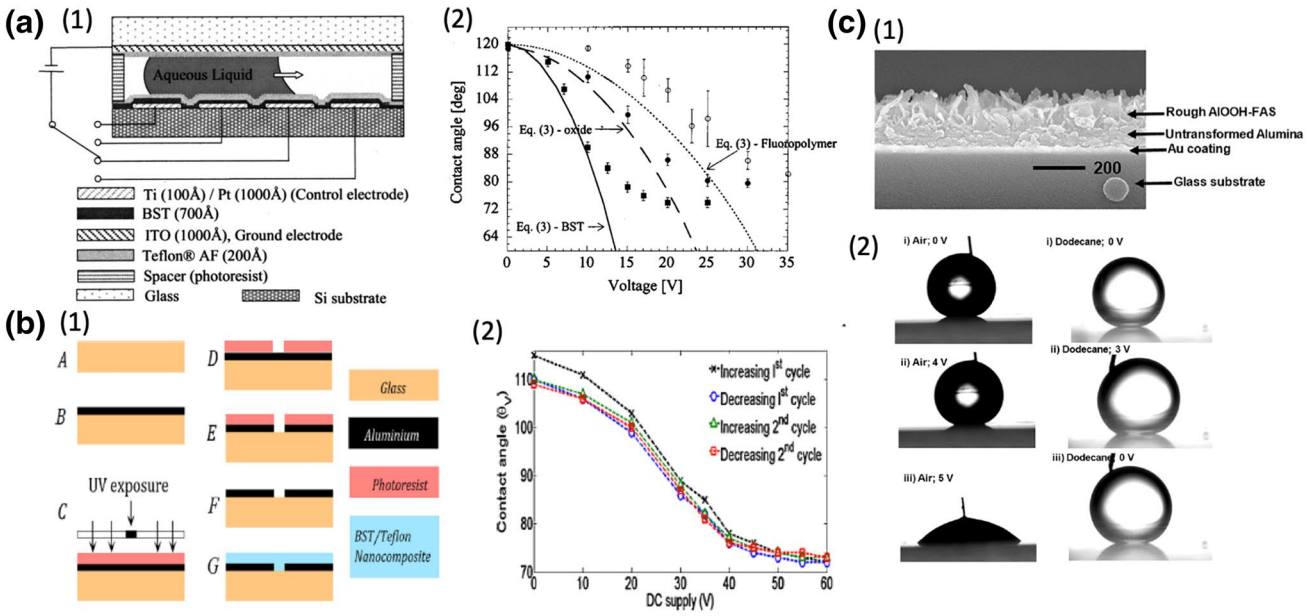

Fig. 2 **a** (1) A coating materials system of barium strontium titanate (BST)-based dielectric layer. (2) The proposed BST coating exhibits a 60° contact angle change with voltage less than 15 V (Moon et al. 2002) **b** (1) A DMF coating which combines BST and Teflon nanocomposite as both dielectric and hydrophobic layers at the same time. (2) The fabricated device shows a 40° contact angle difference under 60 V (Sohail et al. 2016). **c** (1) Modified alumina as high dielectric constant material for DMF application. (2) The droplet performs wetting behavior with only 5 V actuation potential in the air media (Nbelayim et al. 2017)

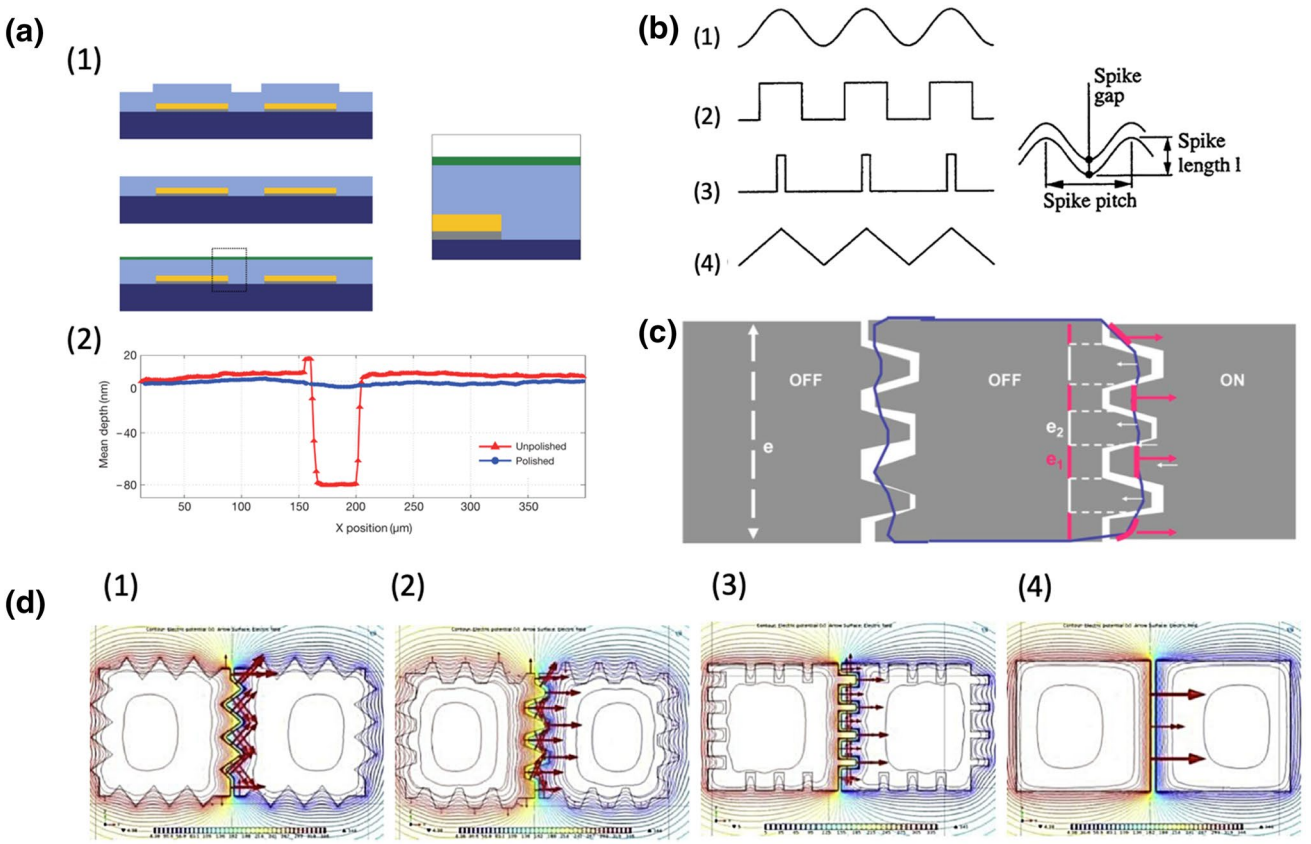

Fig. 3 **a** (1) The Procedure of polishing surface and coating thereafter. (2) The height difference between a polished surface and an unpolished surface (Shirinkami et al. 2017). **b** (1)–(4) Several different types of dented structure (Lienemann et al. 2003). **c** Schematic of the crenelated electrodes and position of the droplet (Berthier et al. 2007). **d** (1)–(4) Simulation of different edge parameters regarding droplet mobility (Jain et al. 2017a)

(Fig. 2a). In their devices, BST is coated through the metalorganic chemical vapor deposition (MOCVD) process at 700 °C with a final thickness of 700 Å. Although BST offers such good dielectric properties, it is really rare to be used in the following DMF devices because of the expensive and high-temperature fabrication process. Most of the substrate and electrode materials will be melted under that kind of condition. To address this issue, another group created a nanocomposite that combines the crystallized BST nano-powders with Teflon, which shows in Fig. 2b (Sohail et al. 2016). The synthesized nanocomposite can be coated on metal electrodes through the spin coating method. This material works as both a dielectric layer and a hydrophobic layer at the same time. The final device performs contact angle change of 33° with 40 V. A multi-layer dielectric coating method reduces the actuation voltage to less than 12.6 V (Samad et al. 2017). Tantalum oxide (TaO_x) also exhibits good potential as a robust and reliable dielectric layer for low-voltage EWOD together with the Cytop hydrophobic layer (Li and Cahill 2017; Mibus and Zangari 2017). A very thin (20 nm) dielectric with only 10 V actuation voltage is achieved by using aluminum as electrodes so that they can passivate at coating defects (Khodayari et al. 2012). In Fig. 2c, a much lower EWOD actuation (less than 5 V) voltage was developed. Reversible electrowetting under 3 V is achieved with rough pseudo-boehmite alumina structures and Nafion through layer-by-layer (LBL) coating (Nbelayim et al. 2017). It has been proved that even lower than 1 V EWOD phenomenon can be observed, but most of them are not reversible, which is not suitable for microfluidic device applications (Liu et al. 2015; Lomax et al. 2016; Maglione et al. 2018).

2.2 Optimization of electrode geometry

The geometry of DMF electrodes, including the height and shape of fabricated electrodes, gaps between adjacent electrodes, and surface properties of coated dielectric and hydrophobic layers, will influence the movement of the droplet in different aspects (Das et al. 2010; Yafia and Najjaran 2013). It is known well that the contact angle hysteresis happens on a rough surface where the liquid tends to propagate

through the nano-structured layer (Krupenkin et al. 2004). A smoother surface is obtained by using fluoropolymer as hydrophobic layer to prevent the droplets from sticking to one electrode (Pollack et al. 2000). Surface polishing process (Fig. 3a) is also introduced to reduce the height difference between electrodes and gaps after coating (Shirinkami et al. 2017). In EWOD microsystems, the gaps between electrodes generate permanent hydrophobic region which will lead to failure movement if the droplet is "confined" within the electrode (Nahar et al. 2016). To address this issue, several types of jagged electrode shapes, including triangle and rectangular (Fig. 3b), have been designed and used in DMFs (Lienemann et al. 2003). In Fig. 3c (Berthier et al. 2007), the electrowetting force along moving direction acts on the droplet in the beginning of motion is described as follows:

$$F_{\mathrm{e,start}} = e_1\gamma\left(\cos\theta_{\mathrm{a}} - \cos\theta_{\mathrm{na}}\right), \tag{2}$$

where e_1 represents the length of contact line on actuated electrodes, γ is solid–liquid surface tension, θ_{a} and θ_{na} are the contact angle on actuated and non-actuated electrodes. For the same device configuration and voltage application, droplets will have longer contact line with its next electrode, which results in larger EWOD force and better movement. A model of criteria for the design of jagged electrodes (Berthier and Peponnet 2007) has also been developed as following equation, which should be larger than 1:

$$G(\lambda, e, \delta, n) = \frac{\lambda/e}{\delta/e + \left[\theta_2/\theta_1 - 1\right]/\pi n}, \tag{3}$$

where λ and n represent dents size and number, e is the width of electrodes, δ is the gap length, θ_1 and θ_2 are contact angle with and without voltage actuation.

The impact of dented electrodes shape has also been evaluated through both finite element modeling and experimental verification (Jain et al. 2017a), which is shown in Fig. 3d. It turns out that zigzag-flat shape will generate a larger driving force on the droplet than other designs. Comparing to covered DMFs with the ground electrode placed on the top plate, the position of the ground electrode in open DMF varies in different configurations. An optimization in the geometry of the ground electrode position in open DMF devices has been studied (Abdelgawad et al. 2009). The proposed design showed about three times of driving force at the beginning of droplet movement than normal configuration. Electrode shape design can also cooperate with the selection and coating of dielectric materials to further decrease minimum actuation voltage (Samad et al. 2015).

3 Alternative powering sources

3.1 Energy harvesting systems

Starting from the beginning of DMF, a high-voltage source is the most common and easy way to achieve an ideal droplet velocity (Cui et al. 2015; Nahar et al. 2016). However, an energy supply equipment and corresponding complicated control unit are required. These extra components largely hinder the development of DMFs to be compact and battery-free devices. Studies have been investigated to reduce the giant energy supply unit in the DMFs. An EWOD device is demonstrated with paint-on liquid–metal electrodes, as shown in Fig. 4a, which exhibits electrowetting phenomenon under the short-circuiting condition (Eaker et al. 2017). In this study, eutectic gallium indium (EGaIn) electrodes were directly painted on a poly(methyl methacrylate) (PMMA) substrate because of the low melting point of EGaIn. The gallium oxide formed on the surface of EGaIn enables tiny voltage EWOD of about 100 mV, which can also be offered through shorting the electrodes to perform a "potential of zero charge" effect. In addition, such a thin passivating oxide layer is strong enough to maintain the film shape of liquid metal, which can be applied on both non-planar and stretchable substrates.

The ability to change mechanical stress into electricity makes piezoelectric material a good candidate to work as a power source of DMFs. Figure 4b shows a DMF device that utilizes the advantages of the piezoelectric phenomenon, where the droplet is actuated through a series of piezoelectric panels (Peng et al. 2014). An output voltage larger than 40 V was obtained, which is adequate to operate droplet by EWOD mechanism. Also, successful droplet merge and split operations have been demonstrated with being actuated by fingers accordingly. The use of piezoelectric material also inspires the possibility of collecting and transferring different types of energy for the DMF power source. An energy harvesting system, which gathers triboelectrification energy to power a DMF device, has been developed (Fig. 4c) (Chen et al. 2018). EWOD phenomenon can be triggered by sliding droplets, which can be obtained from the natural environment, down through the surface of a Teflon-coated panel. Charges will accumulate on the sliding droplet and polarize the Teflon layer, then the corresponding actuation chip gains excessive charge to actuate droplets. Similarly, a DMF device powered by the triboelectric nanogenerator (TENG) was investigated in Fig. 4d (Nie et al. 2018). When manually moving a piece of Kapton film over an array of aluminum foils, the contact electrification generates negative charges on Kapton film. Therefore, same amount of positive charges will be generated on the Al foils accordingly. When the Kapton film is overlapped the second film, negative charges on

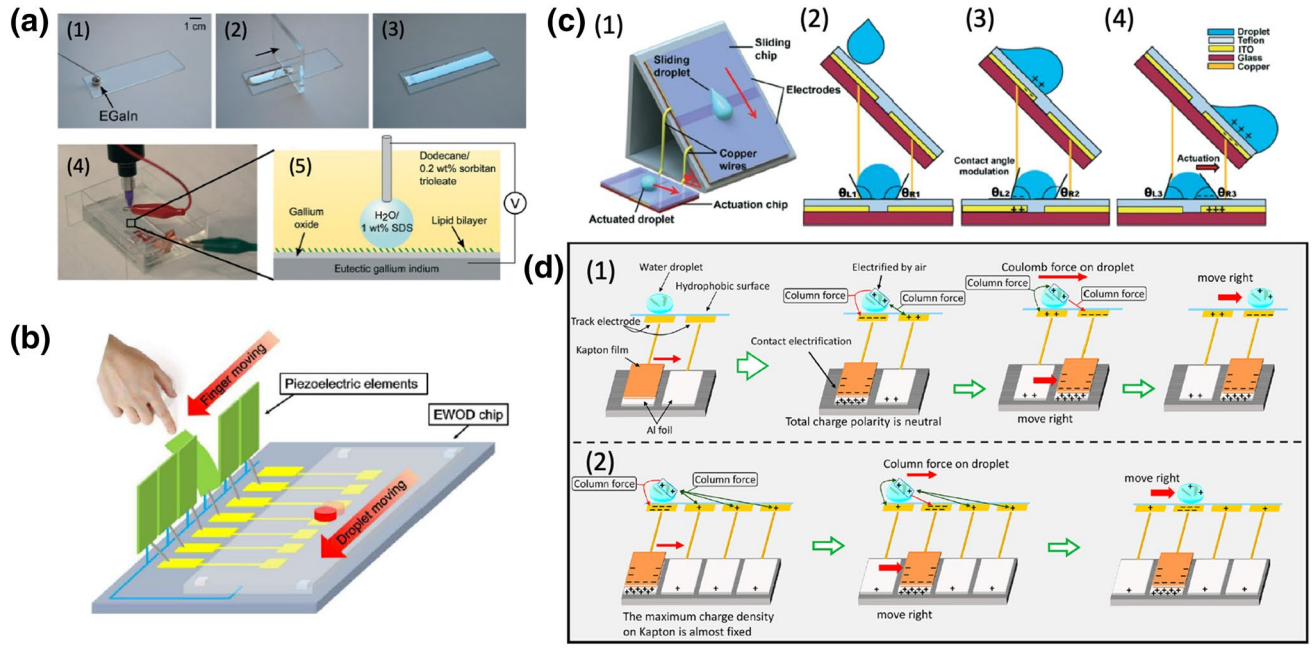

Fig. 4 **a** EWOD devices without external voltage. (1)–(3) Spread a drop of eutectic gallium indium (EGaIn) on a glass substrate to form a film on the surface. (4). (5) Configuration of applying the voltage through a top electrode and the EGaIn layer (Eaker et al. 2017). **b** Piezoelectric triggered droplet movement by bending the corresponding piezoelectric elements (Peng et al. 2014). **c** (1) Energy harvesting DMF configuration. (2)–(4) The droplet is actuated while the other droplet is sliding down the tilted surface (Chen et al. 2018). **d** The droplet is actuated through triboelectric potential generated by a piece of Kapton film and aluminum foils in the case of (1) two electrodes and (2) four electrodes (Nie et al. 2018)

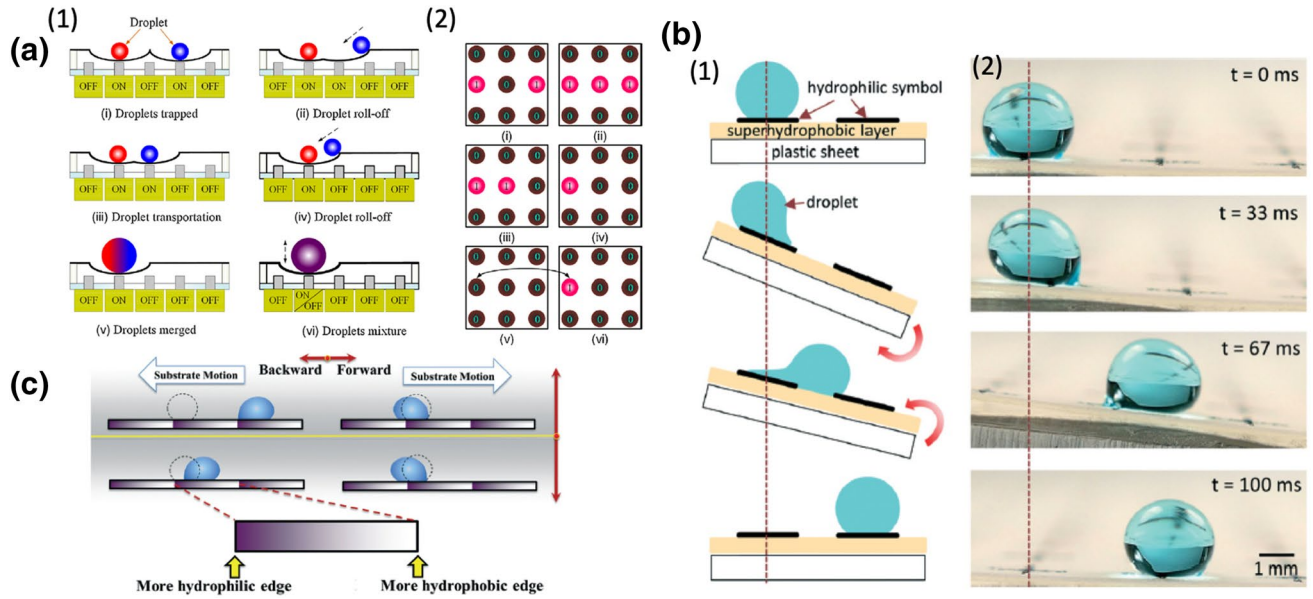

Fig. 5 **a** Mechanism of electromagnetic pillar array manipulated droplet motion. (1)–(2) Droplet behavior with corresponding switch status (Yang et al. 2018). **b** Schematic of droplet transportation leading by substrate rotation. (1)–(2) The fast tilting of the stage enables droplet to move to the next hydrophilic region (Kong et al. 2016). **c** Droplet manipulation with gradient wettability surface. While the plane vibrating, the droplet will overcome the hydrophobic barrier and move the next position (Qi et al. 2019)

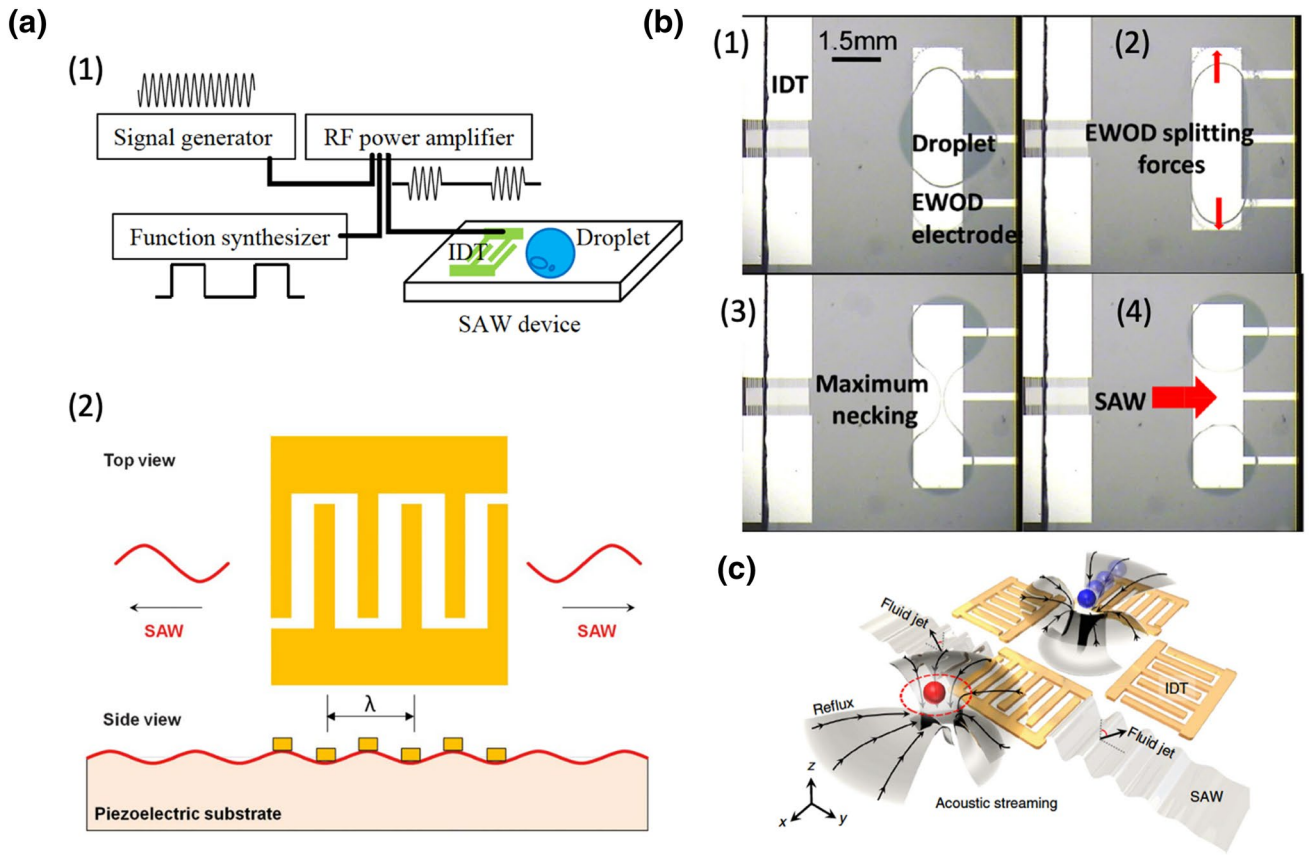

Fig. 6 **a** Mechanism of surface acoustic wave (SAW) DMF devices. (1) A typical system for investigating the SAW phenomenon. (2) Schematic of SAW generation through a metallic interdigitated transducer (IDT) deposited on the piezoelectric substrate (Ding et al. 2013; Kondoh 2018). **b** An integrated DMF device that combines EWOD and SAW mechanisms together to perform a droplet splitting function (Li et al. 2012). **c** A non-contact droplet manipulation unit formed by four IDTs based on SAW technology (Zhang et al. 2018)

the film cannot be fully neutralized by the Al foil, hence negative charges will be generated on the track electrode which is connected to the Al foil. Such negative charges can drive the positively electrified water in the air. The uniqueness of this configuration is that it not only eliminates the requirement for power source, but also eliminates the dielectric layer since the mechanism is no longer the same as EWOD.

3.2 Mechanical actuation platform

The manipulation of droplets in the devices mentioned above depends on the electrostatic force which acts on the droplets more or less (Baird et al. 2007; Young and Mohseni 2008). Biomolecules or cells may suffer from potential influences under those electric fields, which limits the application of DMFs. In such situations, a mechanical actuation method is highly preferred.

A magnetic particles embedded stretchable film has been reported to be used as droplets manipulation platform (Biswas et al. 2016). The surface of such film subjects to deform under external magnetic field changes. Droplets will move toward lower surface area naturally by gravity. Figure 5a shows a similar DMF device which also utilizes the flexible surface (Yang et al. 2018). Differently, a superhydrophobic magnetoelastic film is fabricated as a whole substrate and placed on top of an array of electromagnetic and polydimethylsiloxane (PDMS) pillars. By turning on corresponding switches, the electromagnetic pillars will generate a magnetic field to deform the local upper film, which enables surrounding droplets to move toward this lower area naturally.

Apart from the deformable substrate, a tilted rigid platform has been developed to transport droplets, which is shown in Fig. 5b (Kong et al. 2016). In this configuration, an array of hydrophilic symbols is fabricated on top of a superhydrophobic layer. While tilting the plate, droplets will move to the next hydrophilic region under the gravity and mechanically agitated from the platform. A fast and precise droplet moving step is reported with only 100 ms, and multiple droplets manipulation ability has also demonstrated. Another mechanically actuated DMF with both hydrophobic and hydrophilic surfaces is reported recently (Fig. 5c) (Qi

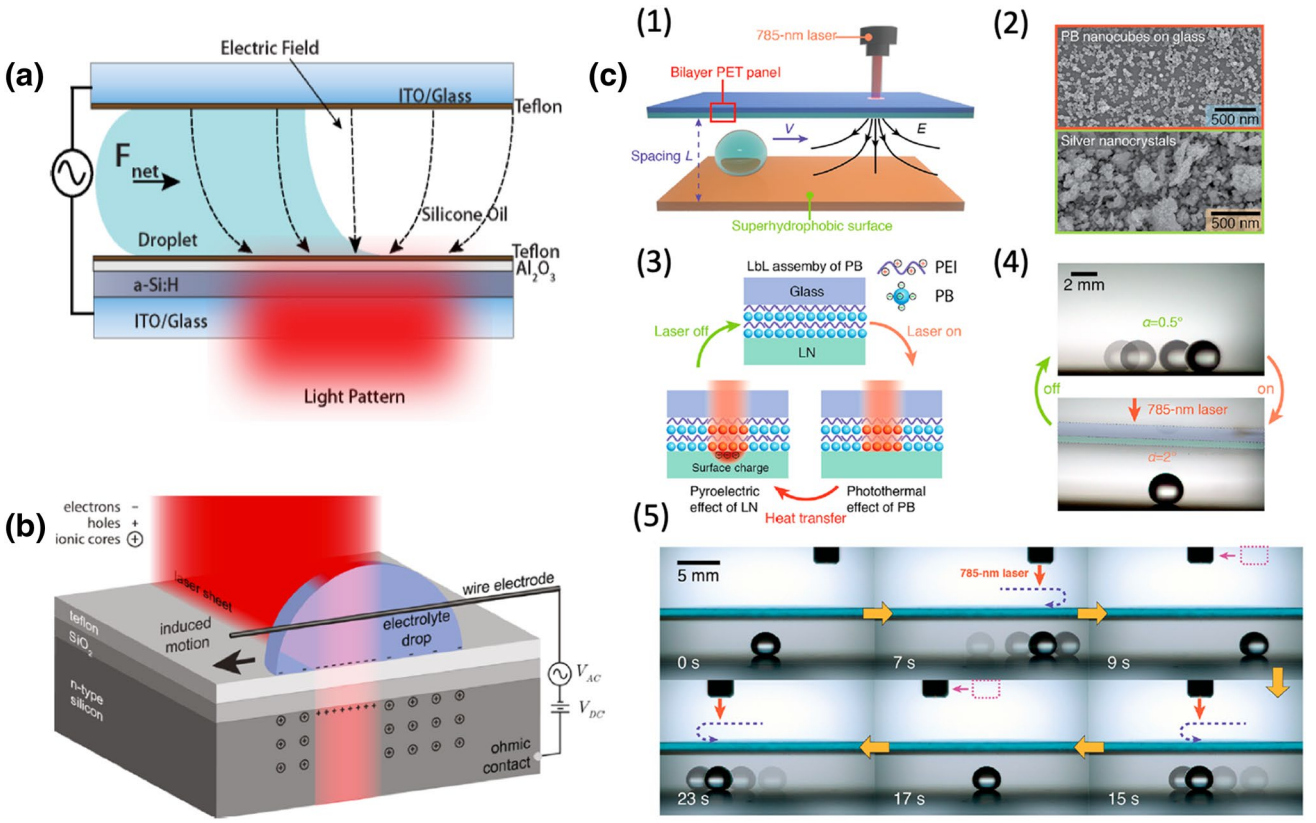

Fig. 7 **a** Mechanism of one type of light-driven DMF. The light changes the conductivity of a-Si:H film, resulting in localized electric field concentration which drives droplet through electro-mechanical force (Pei et al. 2010). **b** Open type DMF driven by light with catena. A deep depletion layer in the silicon while shining light on part of the region (Palma and Deegan 2018). **c** (1) Configuration of pyroelectro-trapping on the superhydrophobic system. (2) Scanning electron microscope (SEM) images of photothermal Prussian blue (PB) nanocubes (3) The mechanism of light-driven droplets transportation. (4) The droplet sliding angle change with turning on laser light. (5) Consecutive droplet manipulation by 785 nm laser (Tang and Wang 2018)

et al. 2019). In this device, each moving step contains a gradient changed hydrophobic "pixel" which attracts droplet to its hydrophilic end. Under certain frequency of horizontal vibration, the droplet can overcome the hydrophobic barrier and move to the next patch's hydrophilic region. Also, the induced vibration is reported to be able to speed up the reaction time in the protein concentration measurement application.

3.3 Surface acoustic wave devices

Surface acoustic wave (SAW) has been used in different types of devices and sensors for decades (Pohl 2000; Gronewold 2007; Lee et al. 2012; Li et al. 2012; Collins et al. 2013). The advantages of SAW over other types of DMF mechanisms, such as large actuation force, fast fluidic actuation, high biocompatibility, and less complicated electrodes geometry, attract notable attention in recent years (Yeo and Friend 2009; Trung-Dung and Nam-Trung 2010; Ding et al. 2013). Figure 6a shows the basic mechanism of the SAW generation on a microfluidic device (Ding et al. 2013; Kondoh 2018). An interdigitated transducer (IDT) is placed on top of the piezoelectric substrate. When applying a radio frequency (RF) signal to the IDT, acoustic waves will be generated along the direction normal to electrodes because of the change of charge distribution within the piezoelectric substrate, which results in deformation of the material. Longitudinal wave radiation from the substrate to droplet is the driving force in SAW devices. The radiation angle is defined as (Bertoni and Tamir 1973):

$$\theta_{\mathrm{R}} = \sin^{-1} \frac{V_{\mathrm{L}}}{V_{\mathrm{W}}}, \tag{4}$$

where θ_{R} is radiation angle, or known as Rayleigh angle, V_{L} and V_{W} represent the sound velocity of the liquid droplet and phase velocity of SAW.

A droplet driving sequence in SAW usually happened by the propagation of waves along the IDT's direction and "push" the droplet to move away from IDT's location. However, the mechanism of SAW driven DMFs limits part

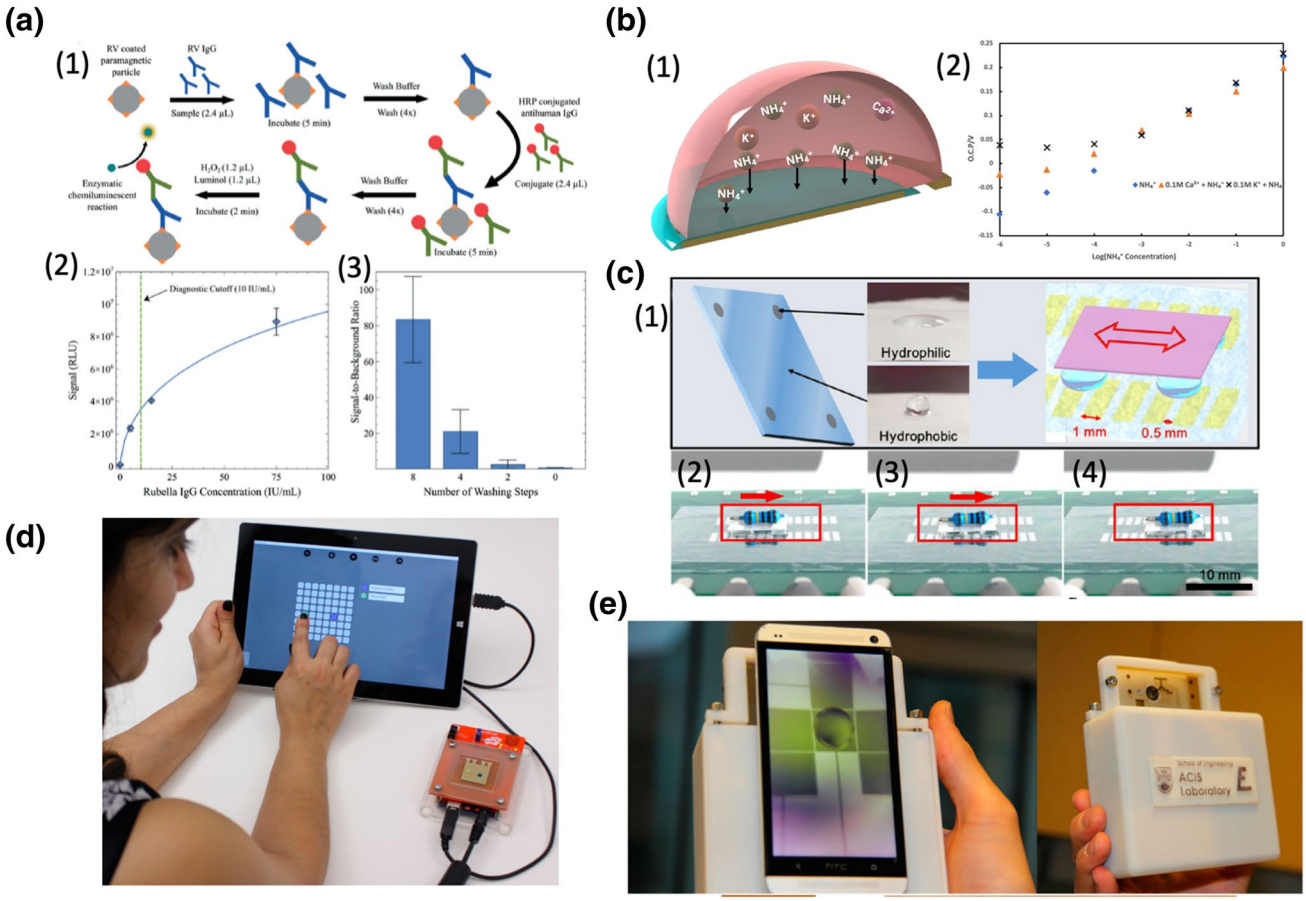

Fig. 8 Applications of DMF devices **a** (1) Schematic of the steps of Rubella virus (RV) immunoglobulin G (IgG) enzyme-linked immunosorbent assay (ELISA) on a DMF platform. (2) RV IgG calibration curve. (3) Effect of the number of washing on the signal intensity (Dixon et al. 2016). **b** (1) Ion-selective sensing mechanism by using an ion-selective membrane (ISM). (2) Selectivity study on an ISM-integrated DMF platform (Min et al. 2019). **c** (1) Schematic of a vehicle formed by four droplets and a piece of Polyvinylidene fluoride (PVDF) electrospinning film. (2)–(4) Sequential images showing the moving sequence of vehicle transportation ability (Nie et al. 2018). **d** A proposed user-friendly interface for a portable DMF platform (Alistar and Gaudenz 2017). **e** A mobile phone-controlled DMF platform with 3D printed case (Yafia et al. 2015a)

of the droplet operations like droplet splitting. Figure 6b shows an integrated system that combines the EWOD electrode with SAW IDTs so that a droplet splitting operation can be obtained, hence the mixing and ejection (Li et al. 2012). The droplet splitting procedure is initiated by applying a voltage on two side electrodes. A maximum "necking" zone will be generated when two droplets achieve saturation status, which can be broken by SAW targeted at the center electrode. The integration of SAW with EWOD not only makes up the shortage of droplet manipulation in the SAW system, but also eliminates the restricted EWOD design constraints to realize the droplet splitting operation. The uniqueness of the propagation property of SAW enables a contactless droplet actuation by separating the droplet from the substrate. In Fig. 6c, a programmable liquid handling device that uses a bio-inert liquid carrier on top of IDT array to carry droplet has been demonstrated (Zhang et al. 2018). In such systems, a thin layer of fluid is applied on the surface of the device. The SAW generated by IDTs propagates along one axis, which pushes the fluid away from the IDTs while the fluid along the perpendicular direction will move toward IDTs to compensate for the loss of fluid, which drives the droplets to move closer to IDTs at the same time. In addition, the generated wave radiation also creates an internal flow within the droplet, so the SAW device will perform a faster droplet mixing comparing to EWOD-type devices (Alghane et al. 2011).

3.4 Light-driven DMFs

The manipulation of discrete droplets is one of the most unique features of DMFs. In a DMF device, the traditional physical "channels" are substituted by an array of 2D electrodes. The mechanisms mentioned above all rely on a well-designed pattern to guide droplets. However, these patterns can also become a barrier for the further development of DMF as they limit the moving area of droplets, and the whole control system will become complicated with the increase of pattern quantities (Zhang and Nguyen 2017). Thus, a "channel-free" DMF will bring more possibilities to the droplet manipulation and the corresponding applications.

Figure 7a shows the mechanism of a light-driven DMF device that removes electrode patterns (Pei et al. 2010). Two pieces of ITO glass are placed parallelly and connected through an AC power source. The droplet is separated from the bottom plate by a layer of a-Si:H, which has high resistivity while no light is illuminated. When a light pattern appears, a-Si:H in the corresponding area becomes conductive. This phenomenon allows external voltage to "pass-through" the oxide and Teflon layers and attracts the droplet to move toward the illuminated region. In recent studies, an open type light-driven DMF, or the photo-electrowetting (PEW) device, which consists of a substrate made from n-type silicon has been reported (Fig. 7b) (Palma and Deegan 2018). A potential difference is pre-applied to droplet and semiconductor, and the generated depletion layer in silicon enables the creation of mobile electron–hole pair under light illumination. Thus, a droplet moving speed of 13 mm/s has been achieved by shining light on part of the droplet. Another loss-free type of light-driven DMF, which is shown in Fig. 7c, has been introduced to address the issue that the partial-wetting surfaces in the previous studies may result in sample cross-contaminations (Tang and Wang 2018). The droplet is placed on top of the superhydrophobic plate, which allows it to move freely. The top plate is formed by Prussian blue (PB) nano-cubes and lithium niobite (LN) coated glass wafer. Under the irradiation of near-infrared (NIR), PB nanocubes generate local heat photothermally. In response to the transferred heat from PB, a non-uniform electric field will be pyroelectrically created by the LN wafer, which attracts the droplets nearby to the radiation spot. Continuous droplet motion can be realized by moving the NIR source around and the electrode-less transportation speed of 1 mm/s has been achieved on such pyroelectro-trapping on superhydrophobic surface (PETOS) platform. The droplet evaporation rate has been evaluated under the condition with and without NIR. It turns out that the temperature of the irradiated droplet remains constant and the evaporation rate under laser illumination will be slightly faster than natural evaporation. The evaporation will not be a critical issue during fast droplet manipulation in such systems.

4 Applications

After the invention of DMFs, the precise manipulation of discrete droplets enables the system to be used for different applications including clinical (Kirby et al. 2014), biology (Wang et al. 2017a), electrochemical sensing (Ruecha et al. 2017), enzyme assays (Fan et al. 2011), etc. For the sensing ability, viscosity, volume, and concentration determining functions can be integrated on DMF chip easily (Li et al. 2014; Tröls et al. 2016). Through

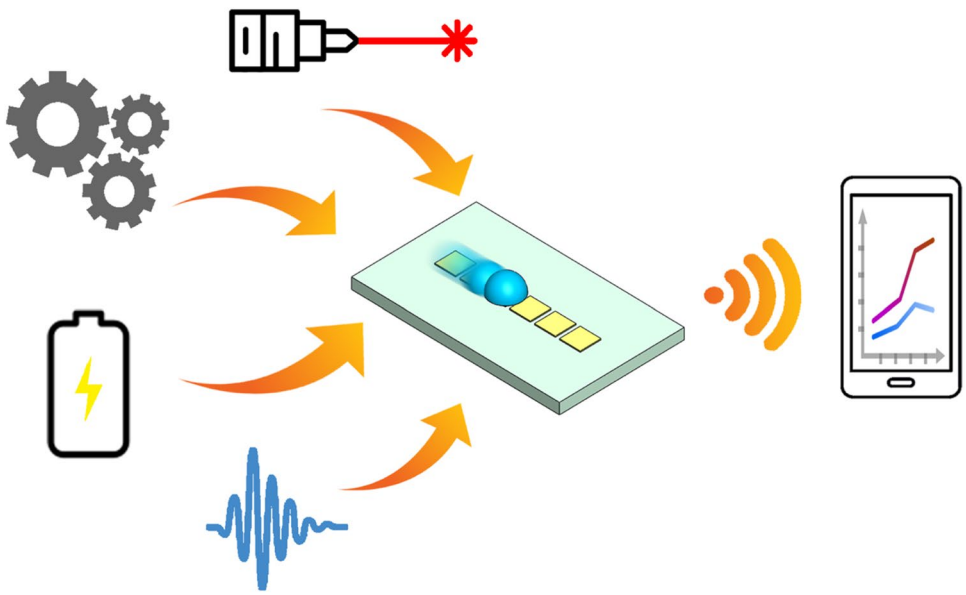

Fig. 9 Schematics of opportunities of DMFs that are powered by alternative sources other than electrical sources such as mechanical, optical, and energy harvesting to power DMF devices to become future portable biochemical assays as an integrated multi-functional lab-on-a-chip application

Table 1 Summary of alternative droplet driving technologies

Droplet actuation technology	Mechanism	Advantages	Disadvantages
Energy harvesting	Actuate the droplet by collecting and converting other types of energy, such as triboelectrification and piezoelectricity	No electric power circuit needed; environment friendly; on-demand operation	Non-programmable droplets actuation
Mechanical actuation	Mechanically deform, tilt, or vibrate the substrate to drive the droplet	No electric field generated; bio-friendly	Require extra components including motors and gearing; complicated "electrodes" design
Surface acoustic wave	Drive the droplet through surface acoustic wave generated from interdigitated transducers, which propagate along the substrate surface	Rapid actuation; simple and efficient operation; high biocompatibility	Limited droplets operations; less droplet moving path flexibility
Light	Generate electric field by specific materials under the shining of light	Electrode-free actuation; high special precision; non-contact feature	Low droplet moving speed; faster droplet evaporation

integrating with multiple reservoirs, a complicated enzymatic detection process can be possible with just a single chip. In Fig. 8a, a heterogeneous Rubella virus (RV) immunoglobulin G (IgG) enzyme-linked immunosorbent assay (ELISA) has been performed with an inkjet-printed DMF device where multiple steps of incubating, washing, and detection can be achieved under precise control of droplet size and location (Dixon et al. 2016). Different types of electrochemical sensors can be integrated on DMF chip easily, which broadens the applications of DMFs to a wide range. Figure 8b demonstrates a DMF platform which has ion-selective sensing capability for the application of a portable soil analyzing equipment (Min et al. 2019). Different from the well-developed chemical and biological applications, a mechanical application of the digital microfluidic device has been introduced recently (Nie et al. 2018). As shown in Fig. 8c, a tiny vehicle was demonstrated with four droplets as "wheels" and a piece of PVDF film as a "body". A maximum load capacity of 500 mg has been achieved, which investigates the field of potential applications of DMF such as drug delivery and liquid robotics. Other applications, such as magnetic-particle-based immunoassays (Choi et al. 2013), gas diffusion control (Ribet et al. 2018), and on-chip heating (Nampoothiri et al. 2018), have been reported, and the huge potential of DMFs as multi-functional platforms have been disclosed.

Although the DMF is claimed to be a promising remote and portable test platform, most of the developed devices still require complicated equipment to assists the detection procedure. Efforts have also been devoted to the design of low energy cost and portable integrated systems. Figure 8d shows a highly compact DMF device, which can be powered and controlled through a laptop, tablet, or smartphone (Alistar and Gaudenz 2017). Another example of DMF device with smartphone application is shown in Fig. 8e (Yafia et al. 2015a). The easy operation property and user-friendly interface lower the barrier of device handling and contribute to the realization of at-home testing.

5 Conclusion and perspectives

This paper considers the unique efforts that have focused to lower the actuation voltage in EWOD-type DMFs and examines the existing alternative mechanisms that have been applied to microfluidic systems. We discussed the material systems used to achieve ultra-low-voltage EWOD devices and a series of efforts on the optimization of device geometry. These studies aim to generate energy-efficient DMF platforms that cater to the lab-on-a-chip concept summarized in Fig. 9. Then, we introduced

and evaluated several DMFs powered by energy sources other than directly applying voltage. The advantage and limitation of each actuation mechanism were discussed individually and a table has been generated to list all the important points of these different types of technologies (Table 1). Although these droplet actuation methods are not that popular or investigated much compared to EWOD-based DMF, the potential and capability of them to work as reliable multi-functional lab-on-a-chip systems have been shown by different studies during past decades.

Despite the advantages owned by different types of DMFs, several aspects need to be improved in future work. Although the extremely low actuation voltage for EWOD-type DMFs has been demonstrated, those materials and electrodes' geometry is not widely used because of the complexity of fabrication steps and cost. A durable and low-cost material system is required to enhance the performance as well as lower the energy consumption of DMFs. Currently, the size of the entire platform is another issue for almost all types of DMF platforms. Even though the dimension of fabricated electrodes can be tens of micrometers, the control unit is still quite large, which limits the portability of the device. The energy harvesting method has the potential to shrink the size of the system, or it is possible to power the device through battery and mobile power after reversible ultra-low-voltage EWOD is achieved. The biological applications with DMFs are still quite rare, which results from cross-contamination along droplets' moving paths on the surface of devices. Efforts have been devoted to developing durable self-cleaning surfaces on DMF devices through nano-structured super-hydrophobic surfaces, disposable polymer films or silicone oil additives. However, none of these methods offer a good balance considering the low cross-contamination, detection convenience, durability, and compatibility with DMF devices.

With all the challenges mentioned above, DMFs are still in improving phase under the cooperation with new droplet actuation methods, materials development, and fabrication technologies. DMF devices will have even broader applications to serve as a portable, multi-functional platform in the future.

References

Abdelgawad M, Park P, Wheeler AR (2009) Optimization of device geometry in single-plate digital microfluidics. J Appl Phys. https://doi.org/10.1063/1.3117216

Alghane M, Chen BX, Fu YQ et al (2011) Experimental and numerical investigation of acoustic streaming excited by using a surface acoustic wave device on a 128° YX-$LiNbO_3$ substrate. J Micromech Microeng. https://doi.org/10.1088/0960-1317/21/1/015005

Alistar M, Gaudenz U (2017) OpenDrop: an integrated do-it-yourself platform for personal use of biochips. Bioengineering 4:45. https://doi.org/10.3390/bioengineering4020045

Baird E, Young P, Mohseni K (2007) Electrostatic force calculation for an EWOD-actuated droplet. Microfluid Nanofluidics 3:635–644. https://doi.org/10.1007/s10404-006-0147-y

Beebe DJ, Mensing GA, Walker GM (2002) Physics and applications of microfluidics in biology. Annu Rev Biomed Eng 4:261–286. https://doi.org/10.1146/annurev.bioeng.4.112601.125916

Berthier J (2013) Digital microfluidics micro-drops and digital microfluidics. Elsevier

Berthier J, Peponnet C (2007) A model for the determination of the dimensions of dents for jagged electrodes in electrowetting on dielectric microsystems. Biomicrofluidics 1:1–9. https://doi.org/10.1063/1.2409626

Berthier J, Dubois P, Clementz P et al (2007) Actuation potentials and capillary forces in electrowetting based microsystems. Sens Actuators A Phys 134:471–479. https://doi.org/10.1016/j.sna.2006.04.050

Bertoni HL, Tamir T (1973) Unified theory of Rayleigh-angle phenomena for acoustic beams at liquid–solid interfaces. Appl Phys 2:157–172. https://doi.org/10.1007/BF00884205

Beyssen D, Le Brizoual L, Elmazria O, Alnot P (2006) Microfluidic device based on surface acoustic wave. Sens Actuators B Chem 118:380–385. https://doi.org/10.1016/j.snb.2006.04.084

Biswas S, Pomeau Y, Chaudhury MK (2016) New drop fluidics enabled by magnetic-field-mediated elastocapillary transduction. Langmuir 32:6860–6870. https://doi.org/10.1021/acs.langmuir.6b01782

Chang JH, Choi DY, You X et al (2010) Low voltage electrowetting on atomic-layer-deposited aluminum oxide. 2010 IEEE 5th Int Conf Nano/Micro Eng Mol Syst NEMS 2010. https://doi.org/10.1109/nems.2010.5592477

Chen G, Liu X, Li S et al (2018) A droplet energy harvesting and actuation system for self-powered digital microfluidics. Lab Chip 18:1026–1034. https://doi.org/10.1039/c7lc01259d

Chiou PY, Moon H, Toshiyoshi H et al (2003) Light actuation of liquid by optoelectrowetting. Sens Actuators A Phys 104:222–228. https://doi.org/10.1016/S0924-4247(03)00024-4

Chiou CH, Jin Shin D, Zhang Y, Wang TH (2013) Topography-assisted electromagnetic platform for blood-to-PCR in a droplet. Biosens Bioelectron 50:91–99. https://doi.org/10.1016/j.bios.2013.06.011

Choi K, Ng AHC, Fobel R et al (2013) Automated digital microfluidic platform for magnetic-particle-based immunoassays with optimization by design of experiments. Anal Chem 85:9638–9646. https://doi.org/10.1021/ac401847x

Collins DJ, Alan T, Helmerson K, Neild A (2013) Surface acoustic waves for on-demand production of picoliter droplets and particle encapsulation. Lab Chip 13:3225–3231. https://doi.org/10.1039/c3lc50372k

Cui W, Zhang M, Duan X et al (2015) Dynamics of electrowetting droplet motion in digital microfluidics systems: from dynamic saturation to device physics. Micromachines 6:778–789. https://doi.org/10.3390/mi6060778

Darhuber AA, Valentino JP, Davis JM et al (2003) Microfluidic actuation by modulation of surface stresses. Appl Phys Lett 82:657–659. https://doi.org/10.1063/1.1537512

Das D, Das S, Biswas K (2010) Effect of electrode geometry on voltage reduction in EWOD based devices. Int Conf Syst Med Biol ICSMB 2010 Proc. https://doi.org/10.1109/icsmb.2010.5735406

Datta P, Dutta A, Majumder R et al (2016) A design of digital microfluidic biochip along with structural and behavioural features in triangular electrode based array. Proc Comput Sci 93:183–190. https://doi.org/10.1016/j.procs.2016.07.199

Ding X, Li P, Lin SCS et al (2013) Surface acoustic wave microfluidics. Lab Chip 13:3626–3649. https://doi.org/10.1039/c3lc50361e

Dittrich PS, Manz A (2005) Single-molecule fluorescence detection in microfluidic channels—the Holy Grail in μtAS? Anal Bioanal Chem 382:1771–1782. https://doi.org/10.1007/s00216-005-3335-9

Dixon C, Ng AHC, Fobel R et al (2016) An inkjet printed, roll-coated digital microfluidic device for inexpensive, miniaturized diagnostic assays. Lab Chip 16:4560–4568. https://doi.org/10.1039/C6LC01064D

Eaker CB, Joshipura ID, Maxwell LR et al (2017) Electrowetting without external voltage using paint-on electrodes. Lab Chip 17:1069–1075. https://doi.org/10.1039/c6lc01500j

Fan SK, Hsieh TH, Lin DY (2009) General digital microfluidic platform manipulating dielectric and conductive droplets by dielectrophoresis and electrowetting. Lab Chip 9:1236–1242. https://doi.org/10.1039/b816535a

Fan SK, Yang H, Hsu W (2011) Droplet-on-a-wristband: chip-to-chip digital microfluidic interfaces between replaceable and flexible electrowetting modules. Lab Chip 11:343–347. https://doi.org/10.1039/c0lc00178c

Gong J, Kim CJ (2008) Direct-referencing two-dimensional-array digital microfluidics using multilayer printed circuit board. J Microelectromech Syst 17:257–264. https://doi.org/10.1109/JMEMS.2007.912698

Grissom D, Curtis C, Windh S et al (2015) An open-source compiler and PCB synthesis tool for digital microfluidic biochips. Integr VLSI J 51:169–193. https://doi.org/10.1016/j.vlsi.2015.01.004

Gronewold TMA (2007) Surface acoustic wave sensors in the bioanalytical field: recent trends and challenges. Anal Chim Acta 603:119–128. https://doi.org/10.1016/j.aca.2007.09.056

Hadwen B, Broder GR, Morganti D et al (2012) Programmable large area digital microfluidic array with integrated droplet sensing for bioassays. Lab Chip 12:3305–3313. https://doi.org/10.1039/c2lc40273d

Islam MA, Tong AY (2017) A numerical study of parallel-plate and open-plate droplet transport in electrowetting-on-dielectrode (EWOD). Numer Heat Transf Part A Appl 71:805–821. https://doi.org/10.1080/10407782.2017.1309217

Jain V, Devarasetty V, Patrikar R (2017a) Effect of electrode geometry on droplet velocity in open EWOD based device for digital microfluidics applications. J Electrostat 87:11–18. https://doi.org/10.1016/j.elstat.2017.02.006

Jain V, Devarasetty V, Patrikar R (2017b) Study of two-dimensional open EWOD system using printed circuit board technology. Glob J Res Eng Electr Electron Eng 17

Jain V, Raj TP, Deshmukh R, Patrikar R (2017c) Design, fabrication and characterization of low cost printed circuit board based EWOD device for digital microfluidics applications. Microsyst Technol 23:389–397. https://doi.org/10.1007/s00542-015-2680-7

Khodayari M, Carballo J, Crane NB (2012) A material system for reliable low voltage anodic electrowetting. Mater Lett 69:96–99. https://doi.org/10.1016/j.matlet.2011.11.060

Kirby AE, Lafrenière NM, Seale B et al (2014) Analysis on the go: quantitation of drugs of abuse in dried urine with digital microfluidics and miniature mass spectrometry. Anal Chem 86:6121–6129. https://doi.org/10.1021/ac5012969

Kondoh J (2018) Nonlinear acoustic phenomena caused by surface acoustic wave and its application to digital microfluidic system. Jpn J Appl Phys 57:1–8. https://doi.org/10.7567/JJAP.57.07LA01

Kong T, Brien R, Njus Z et al (2016) Motorized actuation system to perform droplet operations on printed plastic sheets. Lab Chip 16:1861–1872. https://doi.org/10.1039/c6lc00176a

Krupenkin TN, Taylor JA, Schneider TM, Yang S (2004) From rolling ball to complete wetting: the dynamic tuning of liquids on nanostructured surfaces. Langmuir 20:3824–3827. https://doi.org/10.1021/la036093q

Lee J, Choi YS, Lee Y et al (2012) Rapid and sensitive detection of cardiac markers in human serum using surface acoustic wave immunosensor. Mater Res Soc Symp Proc 1415:165–171. https://doi.org/10.1557/opl.2012.95

Li YJ, Cahill BP (2017) Frequency dependence of low-voltage electrowetting investigated by impedance spectroscopy. Langmuir 33:13139–13147. https://doi.org/10.1021/acs.langmuir.7b03049

Li Y, Fu YQ, Brodie SD et al (2012) Integrated microfluidics system using surface acoustic wave and electrowetting on dielectrics technology. Biomicrofluidics 6:1–9. https://doi.org/10.1063/1.3660198

Li Y, Li H, Baker RJ (2014) Volume and concentration identification by using an electrowetting on dielectric device. 2014 IEEE Dallas Circuits Syst Conf Enabl Internet Things From Sens Serv DCAS 2014. https://doi.org/10.1109/dcas.2014.6965350

Lienemann J, Greiner A, Korvink JG (2003) Electrode shapes for electrowetting arrays. 2003 Nanotechnol Conf Trade Show Nanotech 2003 1:94–97

Liu Y, Liang YE, Sheng YJ, Tsao HK (2015) Ultralow voltage irreversible electrowetting dynamics of an aqueous drop on a stainless steel surface. Langmuir 31:3840–3846. https://doi.org/10.1021/acs.langmuir.5b00411

Lomax DJ, Kant P, Williams AT et al (2016) Ultra-low voltage electrowetting using graphite surfaces. Soft Matter 12:8798–8804. https://doi.org/10.1039/c6sm01565d

Maglione MS, Casalini S, Georgakopoulos S et al (2018) Fluid mixing for low-power 'digital microfluidics' using electroactive molecular monolayers. Small 14:1–7. https://doi.org/10.1002/smll.201703344

Mcdonald JC, Duffy DC, Anderson JR, Chiu DT (2000) Fabrication of microfluidic systems in PDMS. Electrophoreses 21:27–40

Mibus M, Zangari G (2017) Performance and reliability of electrowetting-on-dielectric (EWOD) systems based on tantalum oxide. ACS Appl Mater Interfaces 9:42278–42286. https://doi.org/10.1021/acsami.7b07366

Mibus M, Hu X, Knospe C et al (2016) Failure modes during low-voltage electrowetting. ACS Appl Mater Interfaces 8:15767–15777. https://doi.org/10.1021/acsami.6b02791

Mijatovic D, Eijkel JCT, Van Den Berg A (2005) Technologies for nanofluidic systems: top-down vs. bottom-up—a review. Lab Chip 5:492–500. https://doi.org/10.1039/b416951d

Min X, Bao C, Kim WS (2019) Additively manufactured digital microfluidic platforms for ion-selective sensing. ACS Sens 4:918–923. https://doi.org/10.1021/acssensors.8b01689

Monkkonen L, Edgar JS, Winters D et al (2016) Screen-printed digital microfluidics combined with surface acoustic wave nebulization for hydrogen-deuterium exchange measurements. J Chromatogr A 1439:161–166. https://doi.org/10.1016/j.chroma.2015.12.048

Moon H, Cho SK, Garrell RL, Kim CJ (2002) Low voltage electrowetting-on-dielectric. J Appl Phys 92:4080–4087. https://doi.org/10.1063/1.1504171

Nahar MM, Nikapitiya JB, You SM, Moon H (2016) Droplet velocity in an electrowetting on dielectric digital microfluidic device. Micromachines 7:1–16. https://doi.org/10.3390/mi7040071

Nampoothiri KN, Seshasayee MS, Srinivasan V et al (2018) Direct heating of aqueous droplets using high frequency voltage signals on an EWOD platform. Sens Actuators B Chem 273:862–872. https://doi.org/10.1016/j.snb.2018.06.091

Nbelayim P, Sakamoto H, Kawamura G et al (2017) Preparation of thermally and chemically robust superhydrophobic coating from liquid phase deposition and low voltage reversible electrowetting. Thin Solid Films 636:273–282. https://doi.org/10.1016/j.tsf.2017.06.019

Ng JMK, Stroock AD, Whitesides GM (2002) Components for integrated poly(dimethylsiloxane) microfluidic systems. Electrophoresis 23:3461–3473

Nie J, Ren Z, Shao J et al (2018) Self-powered microfluidic transport system based on triboelectric nanogenerator and electrowetting technique. ACS Nano 12:1491–1499. https://doi.org/10.1021/acsnano.7b08014

Palma C, Deegan RD (2018) Droplet translation actuated by photoelectrowetting. Langmuir 34:3177–3185. https://doi.org/10.1021/acs.langmuir.7b03340

Park JK, Lee SJ, Kang KH (2010a) Fast and reliable droplet transport on single-plate electrowetting on dielectrics using non-floating switching method. Biomicrofluidics 4:1–8. https://doi.org/10.1063/1.3398258

Park SY, Teitell MA, Chiou EPY (2010b) Single-sided continuous optoelectrowetting (SCOEW) for droplet manipulation with light patterns. Lab Chip 10:1655–1661. https://doi.org/10.1039/c001324b

Pei SN, Valley JK, Neale SL et al (2010) Light-actuated digital microfluidics for large-scale, parallel manipulation of arbitrarily sized droplets. In: 2010 IEEE 23rd international conference on micro electro mechanical systems (MEMS), pp 252–255

Peng C, Zhang Z, Kim CJ, Ju YS (2014) EWOD (electrowetting on dielectric) digital microfluidics powered by finger actuation. Lab Chip 14:1117–1122. https://doi.org/10.1039/c3lc51223a

Pohl A (2000) A review of wireless SAW sensors. IEEE Trans Ultras Ferroelectr Freq Control 47:317–332

Pollack MG, Fair RB, Shenderov AD (2000) Electrowetting-based actuation of liquid droplets for microfluidic applications. Appl Phys Lett 77:1725–1726. https://doi.org/10.1063/1.1308534

Pooyan S, Passandideh-Fard M (2018) Investigation of the effect of geometric parameters on EWOD actuation in rectangular microchannels. J Fluids Eng 140:091104. https://doi.org/10.1115/1.4039512

Qi L, Niu Y, Ruck C, Zhao Y (2019) Mechanical-activated digital microfluidics with gradient surface wettability. Lab Chip 19:223–232. https://doi.org/10.1039/c8lc00976g

Ribet F, De Pietro L, Roxhed N, Stemme G (2018) Gas diffusion and evaporation control using EWOD actuation of ionic liquid microdroplets for gas sensing applications. Sens Actuators B Chem 267:647–654. https://doi.org/10.1016/j.snb.2018.04.076

Rudan M (2015) Physics of semiconductor devices. Phys Semicond Devices. https://doi.org/10.1007/978-1-4939-1151-6

Ruecha N, Lee J, Chae H et al (2017) Paper-Based digital microfluidic chip for multiple electrochemical assay operated by a wireless portable control system. Adv Mater Technol 2:1600267. https://doi.org/10.1002/admt.201600267

Samad MF, Kouzani AZ, Rahman MM et al (2015) Design and fabrication of an electrode for low-actuation-voltage electrowetting-on-dielectric devices. Procedia Technol 20:20–25. https://doi.org/10.1016/j.protcy.2015.07.005

Samad MF, Kouzani AZ, Hossain MF et al (2017) Reducing electrowetting-on-dielectric actuation voltage using a novel electrode shape and a multi-layer dielectric coating. Microsyst Technol 23:3005–3013. https://doi.org/10.1007/s00542-016-3087-9

Shirinkami H, Kim J, Lee C et al (2017) Improvement of droplet speed and stability in electrowetting on dielectric devices by surface polishing. Biochip J 11:316–321. https://doi.org/10.1007/s13206-017-1408-4

Sohail S, Mistri EA, Khan A et al (2016) Fabrication and performance study of BST/Teflon nanocomposite thin film for low voltage electrowetting devices. Sens Actuators A Phys 238:122–132. https://doi.org/10.1016/j.sna.2015.11.019

Tan X, Zhou Z, Cheng MMC (2012) Electrowetting on dielectric experiments using graphene. Nanotechnology. https://doi.org/10.1088/0957-4484/23/37/375501

Tang X, Wang L (2018) Loss-free photo-manipulation of droplets by pyroelectro-trapping on superhydrophobic surfaces. ACS Nano 12:8994–9004. https://doi.org/10.1021/acsnano.8b02470

Tröls A, Clara S, Jakoby B (2016) Sensors and actuators A: physical A low-cost viscosity sensor based on electrowetting on dielectrics. Sens Actuators A Phys 244:261–269. https://doi.org/10.1016/j.sna.2016.04.047

Trung-Dung L, Nam-Trung N (2010) Surface acoustic wave driven microfluidics—a review. Micro Nanosyst 1:1–9

Wainright A, Nguyen UT, Bjornson TL, Boone TD (2003) Preconcentration and separation of double-stranded DNA fragments by electrophoresis in plastic microfluidic devices. Electrophoresis 24:3784–3792. https://doi.org/10.1002/elps.200305594

Wang W, Jones TB (2015) Moving droplets between closed and open microfluidic systems. Lab Chip 15:2201–2212. https://doi.org/10.1039/C5LC00014A

Wang L, Duan J, Zhang B, Wang W (2016) Polydimethylsiloxane as dielectric and hydrophobic material in electro-wetting liquid lens. 8th Int Symp Adv Opt Manuf Test Technol Des Manuf Test Micro-Nano-Optical Devices Syst Smart Struct Mater. https://doi.org/10.1117/12.2245707

Wang H, Chen L, Sun L (2017a) Digital microfluidics: a promising technique for biochemical applications. Front Mech Eng 12:1–16. https://doi.org/10.1007/s11465-017-0460-z

Wang J, Hu J, Sun Q et al (2017b) Dielectric and energy storage performances of PVDF-based composites with colossal permittivitied Nd-doped BaTiO3 nanoparticles as the filler. AIP Adv. https://doi.org/10.1063/1.5003292

Whitesides GM (2006) The origins and the future of microfluidics. Nature 442:368–373. https://doi.org/10.1038/nature05058

Yafia M, Najjaran H (2013) High precision control of gap height for enhancing principal digital microfluidics operations. Sens Actuators B Chem 186:343–352. https://doi.org/10.1016/j.snb.2013.06.029

Yafia M, Ahmadi A, Hoorfar M, Najjaran H (2015a) Ultra-portable smartphone controlled integrated digital microfluidic system in a 3D-printed modular assembly. Micromachines 6:1289–1305. https://doi.org/10.3390/mi6091289

Yafia M, Shukla S, Najjaran H (2015b) Fabrication of digital microfluidic devices on flexible paper-based and rigid substrates via screen printing. J Micromech Microeng. https://doi.org/10.1088/0960-1317/25/5/057001

Yang C, Zhang Z, Li G (2018) Programmable droplet manipulation by combining a superhydrophobic magnetic film and an electromagnetic pillar array. Sens Actuators B Chem 262:892–901. https://doi.org/10.1016/j.snb.2018.02.074

Yeo LY, Friend JR (2009) Ultrafast microfluidics using surface acoustic waves. Biomicrofluidics 3:1–23. https://doi.org/10.1063/1.3056040

Young PM, Mohseni K (2008) Calculation of DEP and EWOD forces for application in digital microfluidics. J Fluids Eng 130:081603. https://doi.org/10.1115/1.2956606

Yu P-H, Lai KY-T, Li Z et al (2017) Droplet size-aware high-level synthesis for micro-electrode-dot-array digital microfluidic biochips. IEEE Trans Biomed Circ Syst 11:612–626. https://doi.org/10.1109/tbcas.2017.2653808

Zhang Y, Nguyen NT (2017) Magnetic digital microfluidics—a review. Lab Chip 17:994–1008. https://doi.org/10.1039/c7lc00025a

Zhang Y, Park S, Liu K et al (2011) A surface topography assisted droplet manipulation platform for biomarker detection and pathogen identification. Lab Chip 11:398–406. https://doi.org/10.1039/c0lc00296h

Zhang SP, Lata J, Chen C et al (2018) Digital acoustofluidics enables contactless and programmable liquid handling. Nat Commun 9:1–11. https://doi.org/10.1038/s41467-018-05297-z